15

Superfluid helium based ultracold neutron source for the PIK reactor

© A.P. Serebrov, V.A. Lyamkin, A.K. Fomin, M.S. Onegin

St. Petersburg Nuclear Physics Institute, National Research Center Kurchatov Institute, Gatchina, Russia
e-mail: serebrov_ap@pnpi.nrcki.ru

Received February 1, 2022
Revised March 15, 2022
Accepted March 29, 2022

The PIK reactor at NRC „Kurchatov Institute"−PNPI is going to be equipped with a high-flux Ultra Cold Neutron (UCN) source for fundamental physics researches. The UCN source will use superfluid helium, which will make possible to achieve the density of UCN $2.2 \cdot 10^3\,\mathrm{cm}^{-3}$, that has not yet been achieved anywhere in the world. The UCN source will be installed on the GEK-4 channel, which will make possible to obtain a low value of heat influx to cryogenic vessels from reactor radiation. The heat removal from the UCN source vessel will be implemented by using a heat exchanger. The calculated UCN density in the EDM spectrometer chamber at the PIK is going to be $200\,\mathrm{cm}^{-3}$, which is 20 times higher than the existing UCN densities in the world. For a new UCN source based on superfluid helium, an extensive research program has been developed in field of the physics of fundamental interactions, including the search for a nonzero neutron EDM, precision measurement of the neutron lifetime, and search for mirror dark matter.

Keywords: ultracold neutrons, neutron sources, superfluid helium, neutron EDM, neutron decay.

DOI: 10.21883/TP.2022.06.54425.21-22

Introduction

The experiments for investigating the properties of the neutron itself require the neutrons to be as slow as possible. When the neutron energy is below a boundary energy of the substance, the neutron can not penetrate the substance and it is reflected from the surface, thereby increasing the residence time of the neutron inside an experimental unit. The surface reflectivity of the ultra cold neutrons (UCN) allows storing them in a closed material volume. The UCNs can be also stored in magnetic traps of a complicated multi-pole shape by interacting the neutron magnetic moment with the magnetic field [1].

The fundamental physics applies the UCNs for measuring the electric dipole moment and the lifetime of the neutron itself. These studies were started in the 1970s in PNPI in the WWR-M reactor to be continued in the ILL reactor, and they were globally the most accurate [2] up to having new results of searching the electric dipole moment (EDM) of the neutron in PSI [3] and measuring the lifetime of the neutron in LANL [4]. These experiments and planned precision correlation researches of the neutron β-decay are crucial for the physics of fundamental interactions: they are correlated to solving the problems of Standard Model (SM) when describing the CP violation and explaining cosmological facts (baryon asymmetry of the Universe). Presently, the interest to measurements of the neutron lifetime is also large due to the fact that there is divergence in the results of the UCN storage experiments and the beam experiments [5,6]. That is why this scientific area (applying the UCNs for studying the fundamental interactions) is actively developing now.

The number of the cold neutrons can be increased by passing the reactor neutrons through a cold retarder. The low-temperature medium can have a portion of the UCNs increased in dozens and hundred times. This method has been already used for producing the UCNs for 50 years. However, despite the active technological advancement, there is still no significant progress in increase in the UCN density for the last 30 years. The thing is that direct and quite effective methods have been already utilized using liquid hydrogen and deuterium at the temperature of 20 K. In 1986, the densities of several dozens of UCNs per a cubic centimeter were obtained at the universal channel source of the WWR-M reactor in Gatchina [7] and in the ILL reactor in Grenoble [8]. The PNPI has also investigated the methods of obtaining the high UCN densities using the solid deuterium. This method of obtaining the UCNs using the solid deuterium at the temperature of 4 K was introduced in PSI [9] and LANL [10].

The further progress requires alternative methods of obtaining the UCNs, for example, using the superfluid helium at the temperature of 1 K. This method is based on the effect of the UCN accumulation in superfluid helium due to features of this quantum liquid [11].

1. Project of the UCN source at the PIK reactor

It is not a new idea of creating the UCN source on the PIK reactor. Essentially, it is its implementation that started in the WWR-M reactor already at the beginning of the 1980s. In this regard, the WWR-M reactor was equipped with the universal channel for polarized cold and ultra cold neutrons. The problem was to obtain experience

in developing the sources of cold and ultra cold neutrons and to extend the research program. The channel was provided with a set of plants to investigate the neutron decay and measure the electric dipole moment of the neutron. In its essence, it was a prototype of an experimental complex, which is planned to be realized now in the GEK-3 channel of the PIK reactor. Although, the researches in the WWR-M reactor have obtained the most important results, relevance of the set physical problems is still growing. The new researches in the PIK reactor enable increasing the measurement accuracy by increasing the neutron efficiency and developing more advanced plants.

The UCN source based on the superfluid helium had been already developed for the WWR-M reactor since 2005 to 2010.The reactor was provided with ideal conditions for obtaining the maximum UCN capacity. On the one hand, we have a core-adjacent thermal column of the WWR-M reactor with a channel diameter of 1 m. It can be used to install thick gamma-radiation lead protection, the graphite retarder, the liquid-deuterium pre-retarder and, finally, the superfluid helium convertor of the 35 l volume, therein. On the other hand, in order to realize the project, the most state-of-the-art cryogenic and vacuum equipment was purchased and put into operation: the L-280 helium liquefier of the capacity of 80 l/h, the helium refrigerator of the capacity of 3000 W @ 20 K, and the vacuum helium vapor pumping system of the capacity of 3 g/s @ 50 Pa. The Monte-Carlo calculations of the UCN density for this source show that it is possible to reach the UCN density of 10^4 cm^{-3} [12] in the EDM-spectrometer trap, whereas in the available UCN sources this density reaches the value of about 10 cm^{-3}. Thus, it is possible to obtain a gain factor of 1000 times.

For the next ten years the WWR-M reactor had been used to fully prove the technology of producing and keeping the helium in a superfluid state under the constant influx heat load. For these purposes, the cryogenic body of the WWR-M reactor was equipped with the full-scale model of the UCN source, which was subsequently started. The experiments with the full-scale model of the UCN source have provided real temperatures of the superfluid helium under the heat load up to 60 W [13], while the design value of the heat load of the WWR-M reactor is estimated to be 30 W. The full-scale model was operated so as to get real experience in handling the superfluid helium, and, most importantly, it has experimentally proven the possibility of keeping helium in the superfluid phase under the constant reactor heat influx.

In 2020, it started implementation of a program for creating the instrument experimental base for the PIK reactor. One of the main instrument complexes in this program was a new UCN source designed to make investigations of the physics of fundamental interactions.

The difference between the sources for the PIK and WWR-M reactor (shown on Fig. 1 and in Table 1) is exactly that the UCN source based on superfluid helium can be placed on the PIK reactor only at the output neutron beam,

Table 1. Main characteristics of the UCN sources on the WWR-M and PIK reactors

Parameter	WWR-M	PIK
Reactor power, MW	16	100
Averaged flux of cold neutrons to HeII, cm$^{-2} \cdot$ s^{-1}Å^{-1}	$3 \cdot 10^{10}$	$1.1 \cdot 10^9$
UCN density in HeII, cm^{-3}	10^4	$2.1 \cdot 10^3$
Parameters of the lead screen:		
temperature, K	300	300
heat release, W	15 000	267
Parameters of the pre-retarder (LD2):		
temperature, K	20	20
heat release, W	287	10.7
Parameters of the converter (HeII):		
temperature, K	1.2	1
heat release, W	37	3.85

whereas the WWR-M reactor enables installation of the superfluid helium chamber directly into the thermal column at the core distance of 40 cm. At the same time, transition from the thermal column to the output beam directly results in loss of the initial density of the neutron flux in proportion to a beam solid angle in relation to 4π.

This beam solid angle factor is about 10^{-4} at the 3 m distance to the neutron source. It is extremely difficult to compensate this factor. The thermal neutron flux of the WWR-M reactor is 10^{14} cm$^{-2} \cdot$ s^{-1}, while the respective thermal neutron flux for the PIK reactor — $7 \cdot 10^{14}$ cm$^{-2} \cdot$ s^{-1}. Thus, in transition of the PIK reactor to the UCN source diagram, the output beam losses four orders of the value due to the beam solid angle. But it can compensate only two orders of the value by the high neutron flux in the PIK reactor.

The UCN output in the source can be increased by reducing the temperature of superfluid helium, thereby increasing the neutron lifetime in the UCN source chamber. Since the total neutron flux to the UCN source chamber will lower, the total heat release in the PIK project will be by an order less than in the WWR-M reactor. The heat influx reduction enables using a cooling diagram of the UCN source chamber cooling diagram by means of a heat exchanger, thereby eliminating mixability of the isotope-clean helium with the natural one. Moreover, the lower neutron flux in comparison with the WWR-M reactor flux enables using the stainless steel as a material for the UCN source chamber, thereby substantially facilitating manufacturing of and adding the reliability to welded structures.

The UCN source will be installed on the biggest one of the available experimental channels of the PIK reactor — the horizontal experimental GEK-4 channel of the diameter of 220 mm. The optimal arrangement of the GEK-4 channel

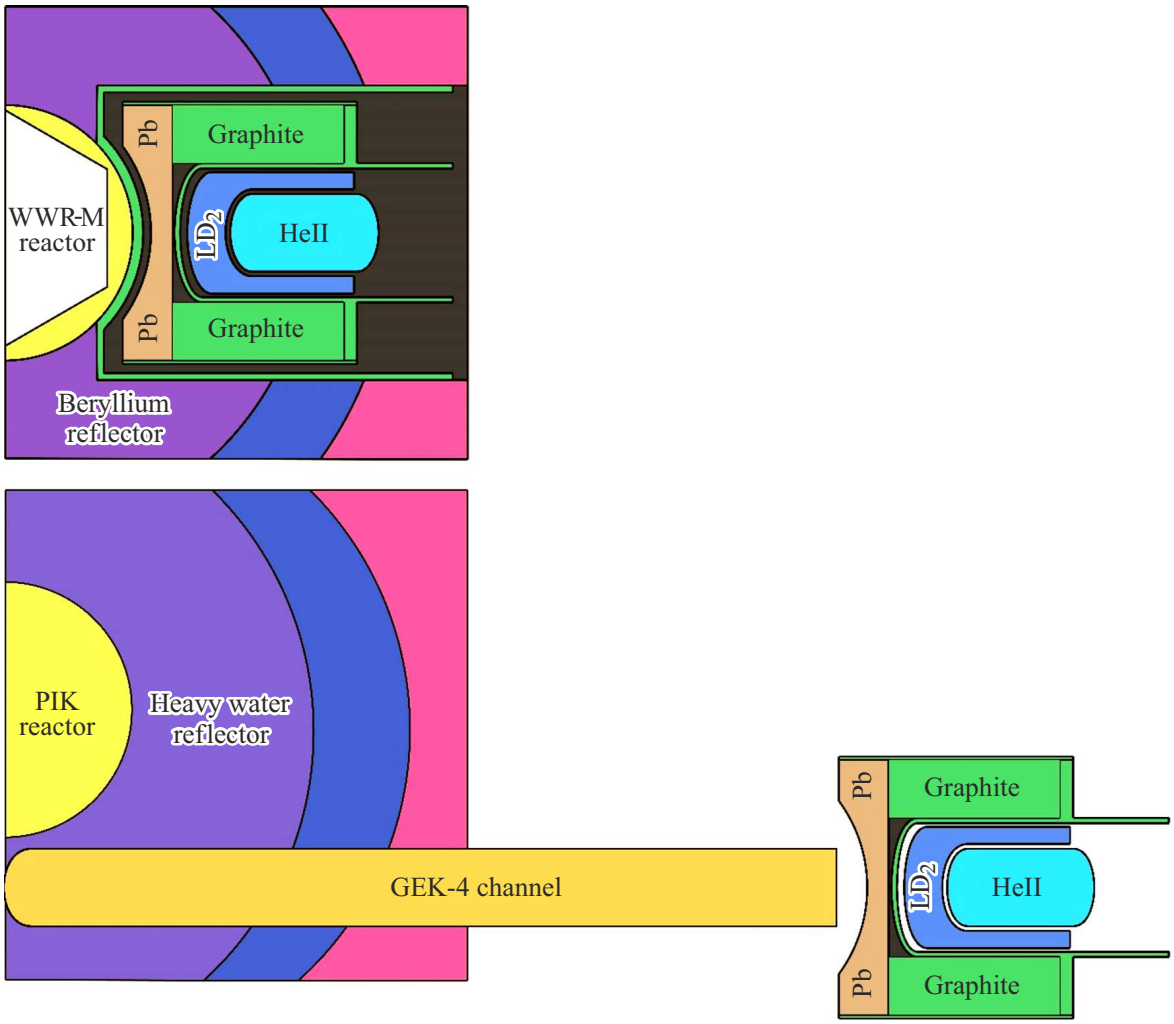

Figure 1. Comparative diagrams of the UCN sources on the WWR-M and PIK reactors.

bottom is on the vertical axis passing through the core center, as it is shown on Fig. 1. The niche of the demountable biological protection shall be provided with a channel of the 1000 mm diameter, which follows the geometry of the vacuum module of the UCN source. The density of the thermal neutron flux at the channel output is expected to be at $6.6 \cdot 10^{10}\,\mathrm{cm}^{-2} \cdot \mathrm{s}^{-1}$.

As in the WWR-M reactor project, the nose part of the UCN source is adjacent to a flange of the GEK-4 channel of the 3 m length. The nose part should include the graphite retarder, the low-temperature pre-retarder and the superfluid helium neutron convertor.

The materials of the pre-retarder were considered to be liquid deuterium and solid methane. The preliminary calculations have shown that the liquid hydrogen pre-retarder provides a substantially lower density of the 9 Å neutron flux in the source at the same heat influxes, and it will not be further considered. The work of optimization of the UCN source has included the so-called inverse diagram of the pre-retarder, which is shown on Fig. 2, *b*. This diagram shows the low-temperature pre-retarder as a reflector designed to return the retarded cold neutrons to the superfluid helium chamber.

The calculations have provided the averaged densities of the neutron fluxes within the helium volume and heat influxes to the main elements of the UCN source. The calculation results for optimization and selection of the pre-retarder material are shown in Table 2. Using the solid methane in the inverse diagram of the pre-retarder provides for the density of the flux of the 9 Å neutrons, which is higher by 65% than the liquid-deuterium pre-retarder in the direct diagram. However, using the solid methane is undesirable in terms of safety. Clogging the cavities with solid methane can result in rupture of the structural elements of the pre-retarder.

The low energy releases in the lead screen allow using non-water coolants for cooling the structure. It has been calculated that using the gas helium as the coolant will increase the density of the flux of 9 Å neutrons in the source in 1.5 times.

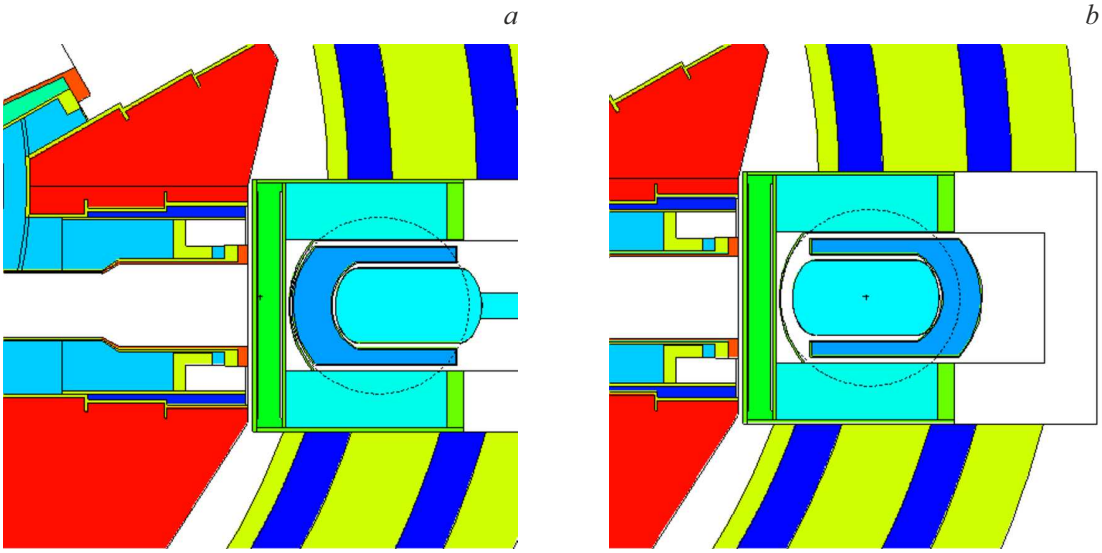

Figure 2. Direct (*a*) and inverse (*b*) diagrams of the UCN source.

Table 2. Calculations for optimization of the UCN source for the PIK reactor

Pre-retarder	Density of the flux of thermal neutrons, $cm^{-2} \cdot s^{-1}$	Density of the flux of the 9 Å neutrons, $cm^{-2} \cdot s^{-1} Å^{-1}$	Energy release in the helium chamber, W	Energy release in the chamber of the pre-retarder, W	Energy release in the lead screen, W
LD_2, orto (the direct diagram)	$6.6 \cdot 10^{10}$ (±2.7%)	$1.1 \cdot 10^{9}$ (±5%)	3.85 (±7%)	10.7 (±4%)	267 (±3%)
LD_2, orto (the inverse diagram)	$1.31 \cdot 10^{11}$ (±2%)	$8.7 \cdot 10^{8}$ (±5%)	4.64 (±4%)	9.3 (±4%)	251 (±2%)
sCH_4 (the direct diagram)	$3.1 \cdot 10^{8}$ (±18%)	$6.0 \cdot 10^{6}$ (±20%)	1.83 (±15%)	11.1 (±10%)	260 (±6%)
sCH_4 (the inverse diagram)	$1.1 \cdot 10^{11}$ (±2.4%)	$1.5 \cdot 10^{9}$ (±3%)	5.53 (±5%)	13.7 (±4%)	262 (±3%)

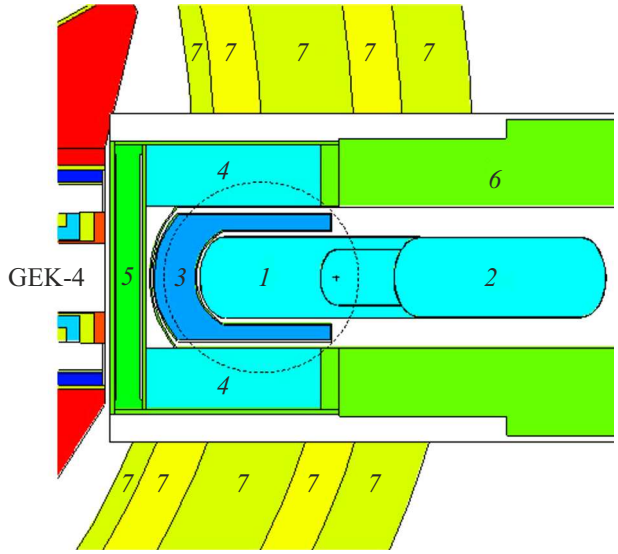

Figure 3. Diagram of the optimized UCN source. Explanations are given in the text.

The optimum design of the nose part of the UCN source for the PIK reactor is shown on Fig. 3. The main elements of the nose part include:

1. Converter — the vessel with superfluid helium at the temperature of 1 K. The converter chamber is made of the stainless steel of the 1 mm thickness.

2. Heat exchanger — the vessel with the coolant (the liquid natural helium at the temperature of 1.1 K) for removal of heat from the converter.

3. Pre-retarder — the pre-retarder is selected to be the liquid deuterium, which substantially increases the number of the 9 Å neutrons in the superfluid helium.

4. Reflector — the reflector is graphite designed to return some number of the thermal neutrons back towards the helium chamber.

5. Protective screen — lead of the 10 cm thickness designed to protect the UCN source structures against the gamma quantums.

6. Biological protection — aluminium blocks for protection against shot-through from the PIK reactor. The aluminium was selected instead of iron to reduction activation of the structure, thereby substantially increasing a repairability degree.

7. Biological protection of the PIK reactor.

2. Research program on the new UCN source

The UCNs play a key role in researches of the physics of fundamental interactions by competing with expensive researches on particle accelerators. The UCN sources can be used to implement the extensive research program for the physics of fundamental interactions. Today, there are 9 science centers in the world, which plan creating the experimental plants based on the UCN [8–10,12,14–18]. The accuracy of these experiments is determined by the UCN density in the experimental traps. That is why the creation of the high-intensity sources is prioritized. Nevertheless, for the last decades the UCN studies have encountered a problem of the low density of the existing UCN sources. Presently, the UCN density used in the experiments is about $2-22\,\mathrm{cm}^{-3}$. Figure 4 shows the experimentally measured UCN density, which is provided by the leading UCN sources in the world [19].

The NRC „Kurchatov Institute"–PNPI is creating the high-intensity UCN source for researches of the fundamental physics. The source based on the PIK reactor will use the superfluid helium, thereby obtaining the UCN density of $2.2 \cdot 10^3\,\mathrm{cm}^3$, which has never been obtained globally. The neutron-guide system of the UCN source can support the studies simultaneously on the five experimental stations.

The initial stage of operation is planned so as to equip the UCN source with the available PNPI experimental plants for neutron EDM search and measurement of the lifetime in the gravitational and magnetic traps [20]. Figure 5 designates these science stations as UCN1, UCN2 and UCN3, respectively. These experiments have been simulated during installation of the UCN source based on the superfluid helium to the PIK reactor.

The gravitational spectrometer for measurement of the neutron lifetime (UCN2) is a trap vessel for neutron storage, which is made of the copper semi-cylinder of the 0.7 m radius and the 2 m length, which is longitudinally cut. In order to measure the contribution of an effective frequency of surface encounters, the spectrometer uses modification of the trap geometry — the so-called insert. The low neutron absorption coefficient of the walls of the trap and the insert is provided by coating the surfaces with a hydrogen-free fluorine polymer (fomblin grease UT-18), which has a low neutron capture section. The internal diameter of the neutron guide leading to the UCN2 plant is 140 mm. The path to UCN2 includes two aluminium membranes of the thickness of $100\,\mu$m and the boundary velocity of 3.2 m/s. One membrane separates the UCN source chamber with the isotope-clean helium from the neutron-guide system, while the second one divides the vacuum in the neutron-guide system and in the measurement volume of the spectrometer. The chambers and the neutron guides have an ^{58}NiMo internal deposition with the boundary velocity of 7.8 m/s and the loss factor of $3 \cdot 10^{-4}$.

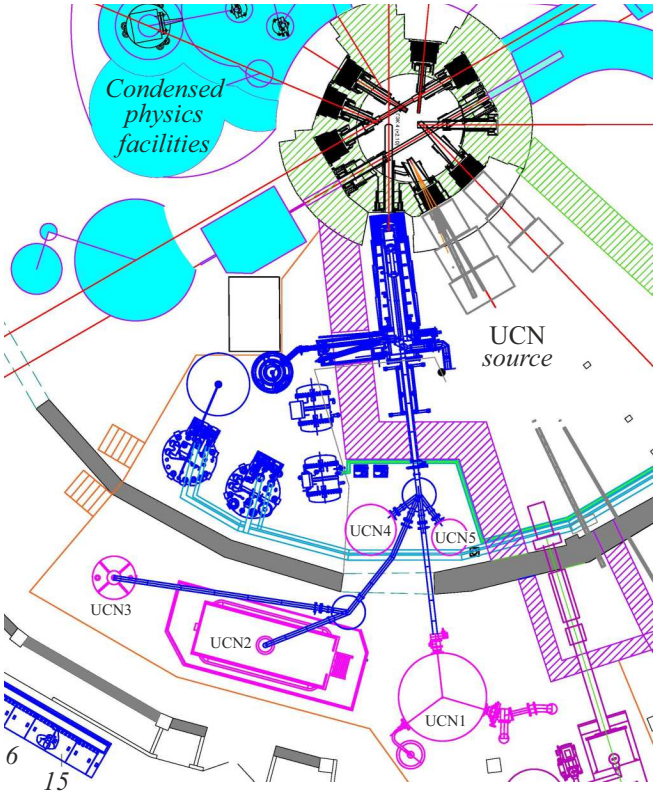

Figure 5. Research program on the UCN source.

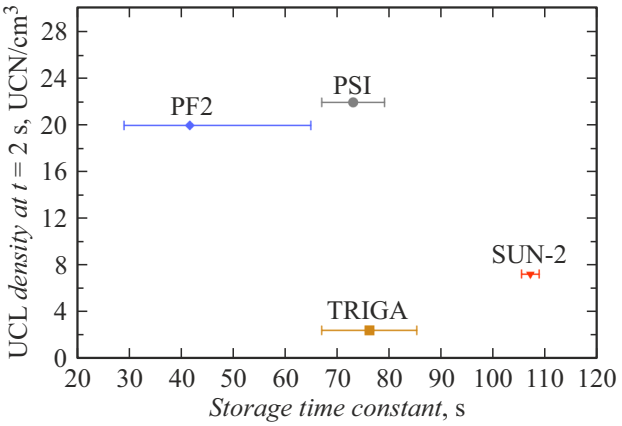

Figure 4. Comparison of the UCN flux density on various reactors: PF2 — Institut Laue-Langevin (France), PSI — Paul Scherrer Institute (Germany), TRIGA — Institute of Nuclear Chemistry (Germany), SUN2 — Institut Laue-Langevin (France).

The simulation was made for the plant designed with a titanium absorber. The developed model specifies the real geometry of the plant and describes the whole experimental procedure. The surfaces of the trap, the insert and the vacuum volume are coated with the polymer fomblin grease UT-18 with the boundary velocity of 4.85 m/s and the loss factor of $8 \cdot 10^{-6}$. The neutron reflections from the neutron guide walls are chiefly mirrored, and the diffusion reflection probability is 0.7%. When the UCNs are reflected from the walls of the trap, the insert and the vacuum volume, the diffusion reflection probability is 10%. The calculations have shown that the gain factor in calculation of a plant detector

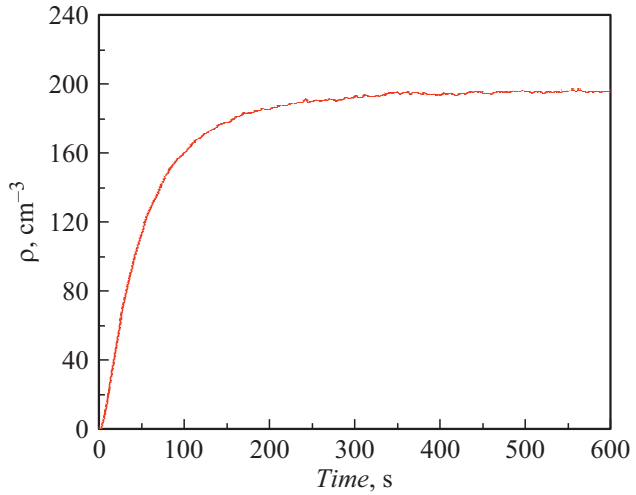

Figure 6. Density in the upper chamber of the EDM spectrometer.

(for measurement of the lifetime in the gravitational trap for the PIK reactor) is at least 16 times in relation to the ILL reactor experiment.

The plant for neutron EDM search (UCN1) is designed as a two-chamber magnetic-resonance spectrometer with the reversible electric field. The spectrometer is characterized by the two chambers available for UCN storage, which have a common system of the magnetic fields, and equal electric fields, which are oppositely directed.

The neutron guide for the EDM spectrometer has the internal diameter of 140 mm, leads straight from the source to be elevated by 700 mm just before the plant entry. Inside the EDM spectrometer, this neutron guide is divided into the two neutron guides, which lead to the two chambers for UCN storage. The source chamber and the neutron guides have an ^{58}NiMo internal deposition with the boundary velocity of 7.8 m/s and the loss factor of $3 \cdot 10^{-4}$. The spectrometer traps have the radius of 263 mm and the height of 76 mm. The boundary velocity of the oxide beryllium coating 6.8 m/s and the loss factor of $1.2 \cdot 10^{-4}$ ensure the neutron storage time at 100 s. The path to UCN1 includes two aluminium membranes of the thickness of 100 μm and the boundary velocity of 3.2 m/s. One membrane separates the UCN source chamber with the isotope-clean helium from the neutron-guide system, while the second one divides the vacuum in the neutron-guide system and in the spectrometer chambers. We discuss an option, which has only one membrane installed at the UCN source output. This case requires very cautious operation of the neutron-guide system, as discharge of the atmosphere into the neutron-guide system by any experimental plant will mean discharge of the atmosphere into the working volume of the EDM spectrometer.

Presently, the safety is prioritized for the UCN source as a whole. It means that the chamber of the UCN source is separated from the spectrometer by two foils. The calculation results of Fig. 6 show that with the two aluminium foils the UCN density in the EDM spectrometer is 200 cm^{-3}. The gain factor is 20 times in relation to the ILL reactor experiment.

Conclusion

Development of a new technology for UCN production is necessitated by the fact that currently there is no progress in increase in the UCN density in the experiments of the physics of fundamental interactions. The thing is that currently, direct and quite effective methods have been utilized using the low-temperature convertors, such as liquid hydrogen or solid deuterium, and further progress requires alternative methods of UCN production. The most promising one of them is a method using the superfluid helium as the converter of cold neutrons into the ultra cold ones.

The new generation of the beam technologies with the high UCN density will allow substantially advancing in the issues of the fundamental studies. By using them, it is assumed to improve the accuracy of neutron EDM measurements by two orders and check predictions of the super-symmetrical theories, which are one of the options of SM expansion. Within these theories, the neutron EDM is predicted to be at the level available for the planned experiments. At the same time, the super-symmetrical theories predict the baryon asymmetry of the Universe at the observed level, which indicates that the proposed options of the theory can be true.

The new UCN source on the PIK reactor can be installed on the GEK-4 channel in the area of small heat influxes to the low-temperature structures of the UCN source. The optimization has resulted in selecting a diagram of heat removal from the UCN source chamber by means of the heat exchanger. The calculated UCN density in the EDM spectrometer chamber on the PIK reactor is 200 cm^{-3} at the UCN density in the closed source chamber equal to $2.1 \cdot 10^3$ cm^{-3}. The gain factor for the UCN density in the EDM spectrometer chamber is 20 times in comparison with other sources, which presently exist.

In addition to the experiment for neutron EDM search, it will be possible to install on the source up to five science stations for the UCN investigations. Currently, an extensive program has been developed for the investigations of the physics of fundamental interactions, including search of the non-zero neutron EDM and precision measurement of the neutron lifetime.

Conflict of interest

The authors declare that they have no conflict of interest.

References

[1] V.K. Ignatovich. *Fizika ultraholodnykh neutronov* (Nauka, M., 1986) (in Russian).

[2] A.P. Serebrov. Phys.-Usp. **58** (11), 1074 (2015). DOI: 10.3367/UFNe.0185. 201511c.1179
[3] C. Abel, S. Afach, N.J. Ayres, C.A. Baker, G. Ban, G. Bison, K. Bodek, V. Bondar, M. Burghoff, E. Chanel, Z. Chowdhuri, P.-J. Chiu, B. Clement, C.B. Crawford, M. Daum, S. Emmenegger, L. Ferraris-Bouchez, M. Fertl, P. Flaux, B. Franke, A. Fratangelo, P. Geltenbort, K. Green, W.C. Griffith, M. van der Grinten, Z.D. Grujić, P.G. Harris, L. Hayen, W. Heil, R. Henneck, V. Hélaine, N. Hild, Z. Hodge, M. Horras, P. Iaydjiev, S.N. Ivanov, M. Kasprzak, Y. Kermaidic, K. Kirch, A. Knecht, P. Knowles, H.-C. Koch, P.A. Koss, S. Komposch, A. Kozela, A. Kraft, J. Krempel, M. Kuźniak, B. Lauss, T. Lefort, Y. Lemiére, A. Leredde, P. Mohanmurthy, A. Mtchedlishvili, M. Musgrave, O. Naviliat-Cuncic, D. Pais, F.M. Piegsa, E. Pierre, G. Pignol, C. Plonka-Spehr, P.N. Prashanth, G. Quéméner, M. Rawlik, D. Rebreyend, I. Rienäcker, D. Ries, S. Roccia, G. Rogel, D. Rozpedzik, A. Schnabel, P. Schmidt-Wellenburg, N. Severijns, D. Shiers, R. Tavakoli Dinani, J.A. Thorne, R. Virot, J. Voigt, A. Weis, E. Wursten, G. Wyszynski, J. Zejma, J. Zenner, G. Zsigmond. Phys. Rev. Lett., **124** (8), 081803 (2020). DOI: 10.1103/PhysRevLett.124.081803
[4] F.M. Gonzalez, E.M. Fries, C. Cude-Woods, T. Bailey, M. Blatnik, L.J. Broussard, N.B. Callahan, J.H. Choi, S.M. Clayton, S.A. Currie, M. Dawid, E.B. Dees, B.W. Filippone, W. Fox, P. Geltenbort, E. George, L. Hayen, K.P. Hickerson, M.A. Hoffbauer, K. Hoffman, A.T. Holley, T.M. Ito, A. Komives, C.-Y. Liu, M. Makela, C.L. Morris, R. Musedinovic, C. O'Shaughnessy, R.W. Pattie, Jr., J. Ramsey, D.J. Salvat, A. Saunders, E.I. Sharapov, S. Slutsky, V. Su, X. Sun, C. Swank, Z. Tang, W. Uhrich, J. Vanderwerp, P. Walstrom, Z. Wang, W. Wei, A.R. Young. Phys. Rev. Lett., **127** (16), 162501 (2021). DOI: 10.1103/PhysRevLett.127.162501
[5] G. L. Green, P. Geltenbort. Sci. Am., **314** (4), 36 (2016). DOI: 10.1038/scientificamerican0416-36. PMID: 27082189
[6] A.P. Serebrov, A.K. Fomin. Phys. Procedia., **17**, 199 (2011). DOI: 10.1016/j.phpro.2011.06.037
[7] I.S. Altarev, N.V. Borovikova, A.P. Bulkin, V.A. Vesna, E.A. Garusov, L.A. Grigor'eva, A.I. Egorov, B.G. Erozolimskii, A.N. Erykalov, A.A. Zakharov, S.N. Ivanov, V.Ya. Kezerashvili, S.G. Kirsanov, E.A. Kolomenskii, K.A. Konoplev, I.A. Kuznetsov, V.M. Lobashev, N.F. Maslov, V.A. Mityukhlyaev, I.S. Okunev, B.G. Peskov, Yu.V. Petrov, P.G. Pikulik, N.A. Pirozhkov, G.D. Porsev, A.P. Serebrov, Yu.V. Sobolev, R.R. Tal'daev, V.A. Shustov, A.F. Shchevetov. JETP Lett., **44** (6), 269 (1986).
[8] A. Steyerl, H. Nagel, F.X. Schreiber, K.A. Steinhauser, R. Gähler, W. Gläser, P. Ageron, J.M. Astruc, W. Drexel, G. Gervais, W. Mampe. Phys. Lett. A, **116** (7), 347 (1986). DOI: 10.1016/0375-9601(86)90587-6
[9] B. Lauss, B. Blau. Sci. Post Phys. Proc., **5**, 4 (2021). DOI: 10.21468/SciPostPhysProc.5.004
[10] T.M. Ito, E.R. Adamek, N.B. Callahan, J.H. Choi, S.M. Clayton, C. Cude-Woods, S. Currie, X. Ding, D.E. Fellers, P. Geltenbort, S.K. Lamoreaux, C.-Y. Liu, S. MacDonald, M. Makela, C.L. Morris, R.W. Pattie, J.C. Ramsey, D.J. Salvat, A. Saunders, E.I. Sharapov, S. Sjue, A.P. Sprow, Z. Tang, H.L. Weaver, W. Wei, A.R. Young. Phys. Rev. C, **97** (1), 012501 (2018). DOI: 10.1103/PhysRevC.97.012501
[11] R. Golub, J.M. Pendlebury. Phys. Lett. A, **62** (5), 337 (1977). DOI: 10.1016/0375-9601(77)90434-0
[12] A.P. Serebrov. Herald Rus. Academy Sci., **79** (1), 14 (2009).
[13] A.P. Serebrov, V.A. Lyamkin, D.V. Prudnikov, A.V. Vasil'ev, K.O. Keshishev, S.T. Boldarev. Tech. Phys., **62** (2), 329 (2017). DOI: 10.1134/S1063784217020256
[14] J. Martin, B. Franke, K. Hatanaka, S. Kawasaki, R. Picker. Nucl. Phys. News, **31** (2), 19 (2021). DOI: 10.1080/10619127.2021.1881367
[15] J. Kahlenberg, D. Ries, K.U. Ross, C. Siemensen, M. Beck, C. Geppert, W. Heil, N. Hild, J. Karch, S. Karpuk, F. Kories, M. Kretschmer, B. Lauss, T. Reich, Y. Sobolev, N. Trautmann. Europ. Phys. J. A, **53**, 226 (2017). DOI: 10.1140/epja/i2017-12428-9
[16] U. Trinks, F.J. Hartmann, S. Paul, W. Schott. Nuclear Instruments and Methods in Physics Research Section A: Accelerators, Spectrometers, Detectors and Associated Equipment, **440** (3), 666 (2000). DOI: 10.1016/S0168-9002(99)01059-1
[17] K.K.H. Leung, G. Muhrer, T. Hügle, T.M. Ito, E.M. Lutz, M. Makela, C.L. Morris, R.W. Pattie Jr., A. Saunders, A.R. Young. J. Appl. Phys., **126**, 224901 (2019). DOI: 10.1063/1.5109879
[18] S. Kavish Imam. Proceed. Sci. **PSTP2019**, 022 (2020). DOI:10.22323/1.379.0022
[19] G. Bison, F. Burri, M. Daum, K. Kirch, J. Krempel, B. Lauss, M. Meier, D. Ries, P. Schmidt-Wellenburg, G. Zsigmond. Res. Section A: Accelerators, Spectrometers, Detectors and Associated Equipment, **830**, 449 (2016). DOI: 10.1016/j.nima.2016.06.025
[20] M.V. Kovalchuk, V.V. Voronin, S.V. Grigoriev, A.P. Serebrov. Crystallography Reports, **66** (2), 195 (2021). DOI: 10.1134/S1063774521020061